CrossMark

Modeling the effect of the cephalic phase of insulin secretion on glucose metabolism

Amparo Güemes[1] (ORCID) · Pau Herrero[1] · Jorge Bondia[2,3] · Pantelis Georgiou[1]

Abstract

The nervous system has a significant impact in glucose homeostasis and endocrine pancreatic secretion in humans, especially during the cephalic phase of insulin release (CPIR); that is, before a meal is absorbed. However, the underlying mechanisms of this neural-pancreatic interaction are not well understood and therefore often neglected, despite their significance to achieving an optimal glucose control. As a result, the dynamics of insulin release from the pancreas are currently described by mathematical models that reproduce the behavior of the β cells using exclusively glucose levels and other hormones as inputs. To bridge this gap, we have combined, for the first time, metabolic and neural mathematical models in a unified system to reproduce to a great extent the ideal glucoregulation observed in healthy subjects. Our results satisfactorily replicate the CPIR and its impact during the post-absorptive phase. Furthermore, the proposed model gives insight into the physiological interaction between the brain and the pancreas in healthy people and suggests the potential of considering the neural information for restoring glucose control in people with diabetes.

Keywords Cephalic phase · Neural modeling · Insulin secretion · Vagus nerve · Metabolic modeling

1 Introduction

Maintaining robust control of glucose homeostasis is essential to guaranteeing the daily function of the human body through the provision of energy in cells via glycolysis. Therefore, to ensure a tight regulation of blood glucose fluctuations our bodies rely on the complex interaction of many organs, such as the pancreas and liver, acting through hormones and neurotransmitters. The brain has also been found to have a crucial role towards this objective [27, 36]. Evidence of its contribution on glucose regulation dates back to the work of the physiologist Claude Bernard, who for the first time showed a causal relationship between brain stimulation of the fourth ventricle in the hindbrain and an increase in plasma glucose levels [13]. Latter research in the field strengthened this evidence by bringing to light the mechanisms that underlie this neural control of glucose homeostasis [17, 27, 35, 41, 42]. However, these findings are just at the beginning of our understanding because most of the neural action schemes are still unknown [27].

Of remarkable interest has always been the study of the implications of central and peripheral neural mechanisms in regulating the endocrine pancreatic function [8, 25, 45, 56]. In particular, the nervous system has been shown to have a major role in the cephalic phase of insulin release (CIPR), which refers to the pre-absorptive secretion of insulin triggered by neural signals rather than to changes in plasma glucose concentrations after meal intake [3, 58]. Between the two major pathways identified in regulating islet secretion, parasympathetic and sympathetic (see Fig. 1), only the former has been found to carry out a significant role in regulating the CPIR [1, 8, 32, 35, 42, 55]. The sympathetic innervation, on the contrary, is not likely to affect CPIR as it mainly inhibits insulin secretion in hypoglycaemia [4, 6, 8, 55]. There are two parasympathetic mechanisms which, through activation of the vagus nerve, enhance insulin and glucagon secretion: (i) cholinergic

✉ Amparo Güemes
amparo.guemes15@imperial.ac.uk

[1] Centre for Bio-Inspired Technology, Department of Electrical and Electronic Engineering, Imperial College London, South Kensington Campus, London, UK

[2] Instituto Universitario de Automática e Informática Industrial, Universitat Politècnica de València, Valencia, Spain

[3] Centro de Investigación Biomédica en Red de Diabetes y Enfermedades Metabólicas Asociadas (CIBERDEM), Madrid, Spain
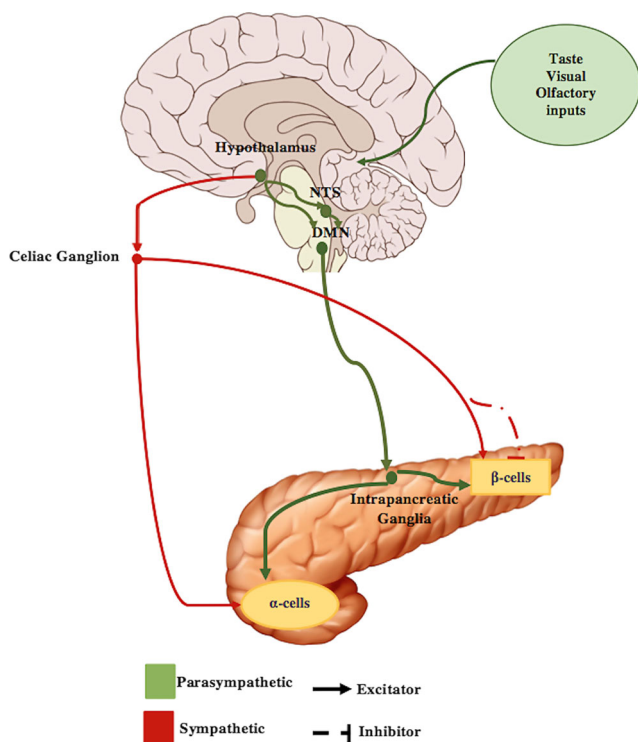
Fig. 1 Diagram depicting the most important neural pathways to the pancreas during the cephalic phase

regulation via release of acetylcholine (ACh) and (ii) non-cholinergic mechanisms mediated by neuropeptides, such as vasoactive intestinal polypeptide (VIP), gastrin releasing peptide (GRP) and pituitary adenylate cyclase activating polypeptide (PACAP) [2, 14]. In some animals, like dogs, rats, and calves, the insulin secretion has been found to be mediated mainly by ACh because it was largely inhibited by atropine, which is a muscarinic antagonist [26]. On the contrary, in humans and pigs, there is evidence of other non-cholinergic neurotransmitters being implicated [3, 26]. The contribution of each parasympathetic mechanism to insulin secretion has been assessed with the use of the ganglionic blocker trimethaphan, which inhibits all the neural transmission to the pancreas [3]. However, the degree of involvement of non-cholinergic mechanisms to the hormonal secretion during the cephalic phase is still not clear [2, 8]. In addition, to the best of our knowledge, there are no reported data describing their release dynamics. Therefore, a mathematical model of the non-cholinergic signaling mechanisms is not available. On the contrary, models of the ACh release after vagal activation have been reported [22, 60]. For these reasons, only the cholinergic mechanism, i.e., through secretion of ACh, is included in the proposed model.

Regarding the characteristics of the CPIR, it lasts up to 10 min and has its peak within the first 4 or 5 min after the food ingestion [3, 47, 49, 52]. Its contribution to the entire

postprandial insulin secretion is quite small, in the range of only the 1 to 3% of the total secretion (approximately 25% above the baseline levels) [47]. It is thought to act mainly on the hepatic glucose metabolism, by allowing a prompt inhibition of gluconeogenesis in the liver [3, 21, 34] and on the metabolism of fats by inhibiting lipolysis [26, 47]. This allows the body to prepare to the rapid and large increase in plasma glucose levels that occurs after meal intake. In addition, absence of the CPIR has been related to an impaired glucose tolerance after a meal through a reduction of postprandial hepatic glucose uptake [3, 21, 37, 46, 47]. Therefore, the CPIR affects the insulin sensitivity, which is a measure of the effectiveness of insulin action on the tissues. To further illustrate its importance, studies in people with type 2 diabetes (T2DM) with an impaired or absent CPIR have reported that injection of a small amount of insulin just after the meal intake resembling the cephalic insulin allowed to successfully increase glucose tolerance in these patients [3, 21, 47]. In conclusion, the resulting effect of the CPIR is a reduction of postprandial glycemic fluctuations and insulin secretion [3, 21, 26, 47].

It is worth noting that the cephalic insulin has not been found to directly affect glucose uptake by other peripheral organs [26].

Existing metabolic mathematical models are implemented using differential equations which describe the cellular dynamics for insulin release from the β cells using exclusively glucose levels and other metabolites as inputs [19, 29, 31]. On the other hand, mathematical models of the neuroregulation of many physiological processes have been developed, including modeling of the respiratory system [43], blood pressure [24], or heart rate among others [22]. However, to the best of our knowledge, models describing the effects of the neural regulation on the pancreatic function have not been reported. Hence, the important neural-pancreatic interaction is currently disregarded, although it is crucial to achieve an optimal glucose control.

To bridge this gap, we have combined for the first time metabolic and neural mathematical models in a unified physiological model to reproduce to a great extent the ideal glucoregulation seen in healthy subjects. This work motivates the development of more comprehensive models of the pancreatic secretion and encourage further investigations on the neural control of glucose homeostasis towards diabetes management.

2 Methods

2.1 The model

Figure 2 depicts the complete scheme of the unified neural-glucose-insulin system model representing the fluxes of
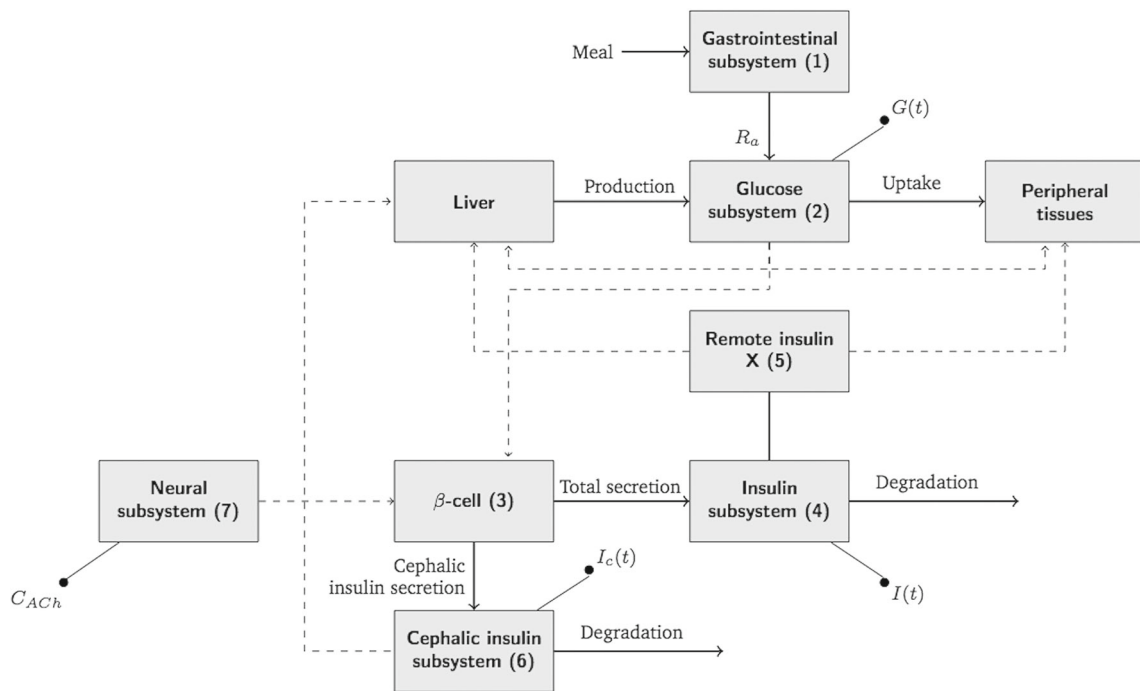
Fig. 2 Diagram of the complete model showing the interaction regarding the mass fluxes (solid lines) and control actions (dashed lines) among the different subsystems (1–7). $I(t)$, $I_c(t)$, and $G(t)$—plasma insulin, plasma cephalic insulin, and plasma glucose, respectively—are the outputs of each subsystem

glucose and insulin and the control actions among them and the brain.

2.1.1 Gastrointestinal absorption model

The amount of carbohydrates taken during a meal is a key input for the glucose subsystem (see block 1 in Fig. 2). The gastrointestinal meal absorption model developed by Hovorka et al. was implemented [29, 31]. This model was selected for two main reasons: (i) its simplicity significantly reduces the number of parameters in comparison with other complex existing models [19], therefore facilitating the complete model identification, and (ii) it has been found to be sufficient to adjust the postprandial glucose profiles of standard meals like the one used in this work [29]. The output of this two-state model is the rate of plasma glucose appearance R_a (mg/min) after an ingestion of a certain amount of carbohydrates D (mg) in a meal. The model is defined by the following equations:

$$\dot{F}(t) = \frac{1}{t_{maxG}}(-F(t) + A_g D \delta(t)), \tag{1}$$

$$\dot{R}_a(t) = \frac{1}{t_{maxG}}(-R_a(t) + F(t)), \tag{2}$$

where $F(t)$ denotes the glucose change in the first compartment, t_{maxG} (min) describes the time-to-maximum of CHO absorption, A_g (unitless) is the carbohydrate bioavailability, and $\delta(t)$ is a Dirac delta.

2.1.2 Glucose subsystem

The model of plasma glucose and insulin interaction developed by Bergman et al. [11] is used as the key subsystem for studying the interaction between insulin and glucose.

The model describes the whole body as a unique compartment with a basal concentration of glucose and insulin. The glucose production and disappearance is influenced by a remote insulin compartment, which is insulin dependent (see interaction among blocks 2 and 5 in Fig. 2).

The model is described by two differential equations:

$$\dot{G}(t) = -[S_G + X(t)]G(t) + S_G G_b + \frac{R_a(t)}{V_G BW}, \tag{3}$$

$$\dot{X}(t) = -p_2 X(t) + p_2 S_I[I(t) - I_b], \tag{4}$$

where $G(t)$ is the plasma glucose concentration; $X(t)$ is the remote active insulin effect on glucose uptake by the tissue and its uptake and production by the liver; p_2 refers to the rate of degradation of the active insulin; BW (kg) is the subject's body weight and V_G (dL/kg) is the glucose distribution volume.

The glucose effectiveness S_G (min^{-1}) is defined as the glucose ability *per se* to promote its own disposal and inhibit its production [29], i.e., independently of insulin. Insulin sensitivity S_I (min^{-1} per pmol/L) is defined as the ability of

insulin to increase glucose effectiveness [29]. As a result, it characterizes the effect of insulin in the balance of glucose production and uptake.

2.1.3 Neural model: ACh secretion

To the extent of our knowledge, there is a lack of *in vivo* experiments in humans regarding the continuous secretion of ACh from the vagus nerve terminals in the endocrine pancreas after vagal stimulation. However, it is reasonable to assume that the kinetics of ACh secretion does not change from one nerve terminal to another. Therefore, in this first proposal, a model based on the ACh secretion by parasympathetic activation on the heart has been used [22, 60]. In particular, the model proposed by Dexter and colleagues [22] was selected.

As reported in the literature, basal insulin secretion is not affected by a blockade of the nervous signaling (e.g., by vagotomy or atropinization) [3, 26]. This is an indicator that there is not significant tonic cholinergic stimulation of the β cells in the fasting state. As a result, only the activation of the vagus nerve terminals elicited by food intake depletes a pool of ACh vesicles, where $0 \leq V(t) \leq 1$ is the normalized quantity of ACh vesicles available for release (dimensionless). The change in ACh concentration in the interstitial space, which is represented by block 7 in Fig. 2, is given by:

$$\dot{V}(t) = -\rho V(t)s(t) + K_R(1-V(t)) \text{ with } V(0) = 1, \quad (5)$$

$$R(t) = m\rho V(t)s(t), \quad (6)$$

$$\dot{C}_{ACh}(t) = -K_D C_{ACh}(t) + R(t) \text{ with } C_{ACh}(0) = 0, \quad (7)$$

where $C_{ACh}(t)$ (nM) represents the interstitial concentration of ACh; K_D (min^{-1}) is the rate of ACh enzymatic degradation; $s(t)$ is the vagal firing patterns or stimulus; K_R (min^{-1}) represents the rate of renewal of vesicles; ρ (unitless) is the fraction of the total vesicles (V) released by each vagal stimulation; and m (nM) is the maximal concentration of ACh that can be released per stimulus.

The real physiological nervous stimulus consists of a burst of action potentials (APs) or spikes (0 or 1 events) with a certain firing frequency, i.e., inter spike time. In order to develop a detailed physiological model, in this work, the nervous stimulus has being modeled as a train of squared pulses ($s(t) = 1$ during the pulse and $s(t) = 0$ otherwise), each of them with a duration δ (ms) that resembles that of the real action potential (see Fig. 6). The activation of the train of pulses occurs in the instant the meal is taken t_{meal} (i.e., as soon as the food is ingested).

Following a first order Boltzmann dynamics, ACh concentration (nM) in the interstitial space eventually reaches a mean plateau value with time (with some superimposed

ripple) that increases with increasing frequencies of stimulation. Only the value at the steady state reflects the action of the neural system, so a simplified version of the neural model considering only the mean concentration of ACh in the steady state was incorporated to the unified neural-metabolic model:

$$V = \frac{K_R}{\rho \, mean(s(t)) + K_R}, \quad (8)$$

$$C_{ACh} = \frac{m \, \rho \, V \, mean(s(t))}{K_D}. \quad (9)$$

This simplified neural model solely depends on the firing frequency of the stimulus, since the higher the frequency, the higher the mean of the stimulus along time, leading to a higher steady-state value for ACh concentration (C_{ACh}).

2.1.4 Insulin secretion

The model used for describing glucose-dependent insulin secretion is based on that proposed by Toffolo et al. [57] and Breda et al. [16], and reported by Dalla Man et al. [19] as:

$$S(t) = \gamma I_{po}(t), \quad (10)$$

$$\dot{I}_{po}(t) = -\gamma I_{po}(t) + I_{p1}(t) + I_{p2}(t) + S_b \text{ with } I_{po}(0) = I_{pob}, \quad (11)$$

$$I_{p1}(t) = \begin{cases} k_{Di}\dot{G}(t) & \text{if } \dot{G} > 0, \\ 0 & \text{otherwise,} \end{cases} \quad (12)$$

$$\dot{I}_{p2}(t) = \begin{cases} -\alpha[I_{p2}(t) - \beta(G(t)-h)] & \text{if } \beta(G(t)-h) \geq -S_b \\ -\alpha[I_{p2}(t) + Sb] & \text{otherwise} \end{cases} I_{p2}(0) = 0 \quad (13)$$

where $S(t)$ (pmol/kg/min) is the total glucose-dependent secreted insulin; γ (min^{-1}) is the transfer rate constant between portal vein and liver $I_{po}(t)$ represents the amount of insulin in the portal vein, subindex b refers to the basal state; $I_{p1}(t)$ (pmol/kg) is responsible for the first phase of secretion, and $I_{p2}(t)$ (pmol/kg) characterises the slower second secretion phase; k_{Di} (pmol/kg per mg/dL) is the pancreatic responsivity to the glucose rate of change; α is the delay between glucose signal and insulin secretion; β (pmol/kg/min per mg/dL) is the pancreatic responsivity to glucose and h (mg/dL) is the threshold level of glucose above which the β cells initiate to produce new insulin. As stated in [19], h has been set to the basal glucose concentration (G_b) to guarantee the steady state in basal conditions.

The pre-absorptive phase of insulin secretion from the β cell is dependent of the interstitial concentration of ACh. In addition, as the literature reports, there is a significant dependence on plasma glucose levels in the effects of ACh on insulin secretion [12, 26]. Both *in vitro* and *in vivo* studies have shown that the effect of ACh is present from 5-nM glucose levels (i.e., normal basal glucose levels) and its

efficacy in insulin release significantly increases with higher glucose levels [12, 26]. Consequently, the novel equations defining ACh action on neurally mediated pre-absorptive insulin release has been defined as:

$$\begin{cases} S_c(t) = \gamma I_{pc}(t), \\ \dot{I}_{pc}(t) = -\gamma I_{pc}(t) + Z(t), \end{cases} \tag{14}$$

$$Z(t) = \begin{cases} K_{ACh} C_{ACh}(t)(G(t) - h) & \text{if } G(t) > h, \\ 0 & \text{otherwise,} \end{cases} \tag{15}$$

where $S_c(t)$ (pmol/kg/min) is the total amount of insulin secreted during the cephalic phase; I_{pc} represents the amount of cephalic insulin in the portal vein, with $I_{pc}(0) = 0$; γ (min^{-1}) is again the transfer rate constant between portal vein and liver; and K_{ACh} (pmol/kg per nM per mg/dL) is the pancreatic responsivity to the ACh interstitial concentration.

As a result, the total amount of insulin secreted by the β-cells, $S_T(t)$ (pmol/kg/min), comprises the glucose-dependent insulin and the insulin elicited by neural stimulation:

$$S_T(t) = S(t) + S_c(t). \tag{16}$$

No delay on the ACh action on cephalic insulin release was included in the proposed model because it was shown to be negligible during the simulations in the time scale of the kinetics of insulin secretion.

2.1.5 Insulin kinetics

The model of insulin kinetics that has been used is based on the two compartment model developed by Dalla Man and colleagues [19]. In this unified neural-metabolic model, it takes the total insulin secretion from the β cell (both glucose and ACh dependent insulin) as an input and determines the plasma insulin. In doing that, it takes into account the insulin degradation rate that occurs in both the liver and the periphery. The set of differential equations that describes this subsystem corresponds to block 4 in Fig. 2 and is the following:

$$\begin{cases} \dot{I}_l(t) = -(m_1 + m_3(t))I_l(t) + m_2 I_p(t) + S_T(t) & I_l(0) = I_{lb}, \\ \dot{I}_p(t) = -(m_2 + m_4)I_p(t) + m_1 I_l(t) & I_p(0) = I_{pb}, \\ I(t) = \frac{I_p}{V_I} & I(0) = I_b, \end{cases} \tag{17}$$

where I_p and I_l (pmol/kg) are insulin masses in plasma and in liver respectively; I (pmol/L) is the plasma insulin concentration; I_b represents the basal state; $S_T(t)$ (pmol/kg/min) is the total insulin secretion form β-cell; V_I (L/kg) is the insulin distribution volume; and $m_1, m_2,$ and m_4 (min^{-1}) are rate parameters. The hepatic extraction of insulin HE, i.e., the insulin flux which leaves

the liver irreversibly divided by the total insulin flux leaving the liver, is time varying [19]:

$$HE(t) = -m_5 S_T(t) + m_6 \text{with } HE(0) = 0, \tag{18}$$

and therefore:

$$m_3(t) = \frac{HE(t)m_1}{1 - HE(t)}. \tag{19}$$

An additional similar block of insulin kinetics but using solely the cephalic insulin secreted (see block 7 in Fig. 2) was included in order to have an independent quantification of its plasma concentration:

$$\begin{cases} \dot{I}_{cl}(t) = -(m_1 + m_3(t))I_{cl}(t) + m_2 I_{cp}(t) + S_c(t) & I_{cl}(0) = 0, \\ \dot{I}_{cp}(t) = -(m_2 + m_4)I_{cp}(t) + m_1 I_{cl}(t) & I_{cp}(0) = 0, \\ I_c(t) = \frac{I_{cp}}{V_I} & I_c(0) = 0. \end{cases} \tag{20}$$

In this way, an independent effect of the part of the total plasma insulin correspondent to the CPIR in the glucose hepatic production can be achieved.

2.1.6 Unified neural-metabolic model: effect of cephalic released insulin

The cephalic insulin acts on the liver causing a prompt inhibition of gluconeogenesis and enhancing the action of postprandial insulin on the hepatic glucose uptake, therefore increasing insulin sensitivity (see Fig. 2) [3, 21, 37, 46]. Hence, in this model the insulin sensitivity changes over time based on the concentrations of the cephalic insulin in plasma $I_c(t)$ (pmol/L):

$$\dot{S}_I(t) = -p_4 S_I(t) + p_4(S_{Ib} + k_{S_I} I_c(t)) S_I(0) = S_{Ib}, \tag{21}$$

where S_{Ib} (min^{-1} per pmol/L) is the basal insulin sensitivity, set to its value when there is no neural control (i.e., $I_c(t) = 0$), k_{S_I} ($\frac{L\ kg}{pmol^2}$) defines the action of the cephalic plasma insulin and p_4 (min^{-1}) is the rate constant describing the dynamics of glucose hepatic production inhibition.

2.2 Experimental data

Experimental data found in the literature were employed for the parameters identification task. The data were extracted from the graphs reported in literature using the software ScanIt [5]. For the identification of the ACh release subsystem, the results obtained by Dexter et al. [22] in a study of the changes in heart rate elicited by vagal stimulation were used (see Fig. 3).

For the rest of the subsystems, the mean results of six female healthy subjects in presence and absence of the ganglionic blocker trimethaphan reported by Ahrén et al. [3] were used (see Fig. 4). The presence of trimethaphan allows achieving a purely metabolic system without any neural
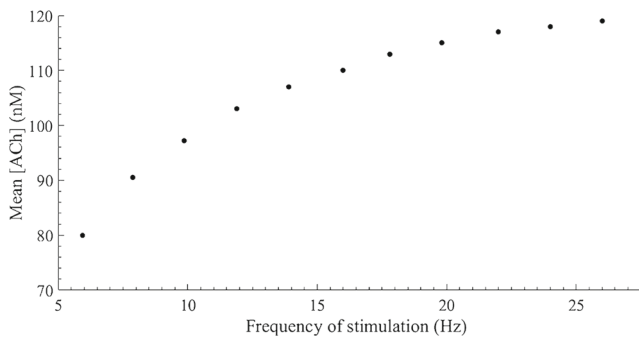
Fig. 3 Mean interstitial concentration of acetylcholine (nM) over time

control, whereas in its absence, the neural contribution is also shown.

2.3 Parameter identification

A sensitivity analysis was carried out to reduce the number of simultaneously identified parameters. Those that had the lowest effect to the system were fixed to their value reported in existing populational models (see Table 2) [19, 22]. In addition, the parameters related with the ACh secretion were fixed to the values defined by Dexter et al. [22] to be consistent with the hypothesis of similar kinetics of release from different vagus nerve terminals. To further reduce the of degrees of freedom and to develop a consistent model, the parameters of each subsystem were progressively identified in three steps by minimizing the coefficient of variation (CV), calculated as the ratio of the root mean squared error (RMSE) to the mean of the dependent variable. An Evolution Strategy with Covariance Matrix Adaptation (CMA-ES) algorithm for nonlinear global optimization was employed [7, 28]. Figure 5 summarizes the identification process and the overall integration of the model.

During the optimization process, the parameters were constrained to lie within a range of values with (i) physiological significance and (ii) lie in the range of values reported in the literature, as shown in Table 1. The final estimation values of the parameters can be found in Table 2. The models were numerically integrated using a RK4 integrator with a fixed integration step size of 0.1 ms for the neural model and 1 min for the unified neural-metabolic model.

3 Results

3.1 Independent neural model identification

The values of the parameters of the independent neural model, including the duration of the pulses identified in the
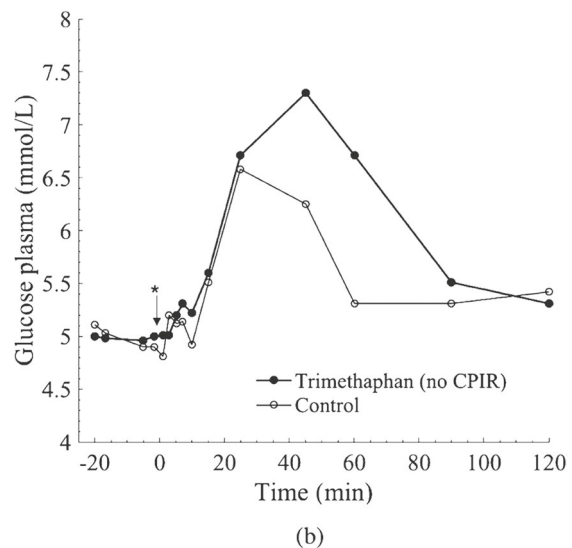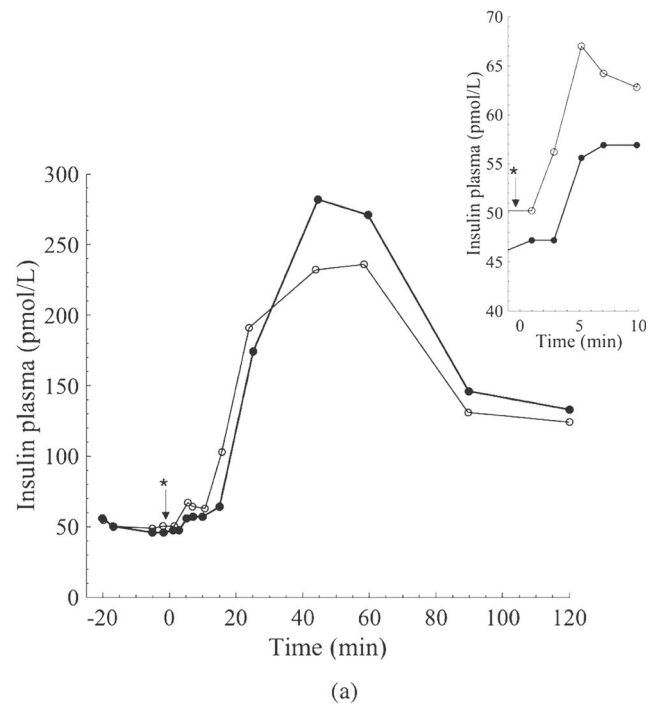

(a)

(b)

Fig. 4 Average serum insulin and plasma glucose levels (N=6). **a** Insulin profile. The small insert shows the insulin levels 10 min after meal intake (depicted with *), which corresponds to the cephalic period. **b** Glucose profile. At time 0 the meal was served

validation process are reported in Table 2. Figure 6 depicts the profiles of vesicles secretion and ACh concentration in the interstitial space, together with the correspondent stimulus, achieved with the independent neural model. To improve the visualisation of the results, an exemplary train of pulses (stimulus) with a firing frequency of
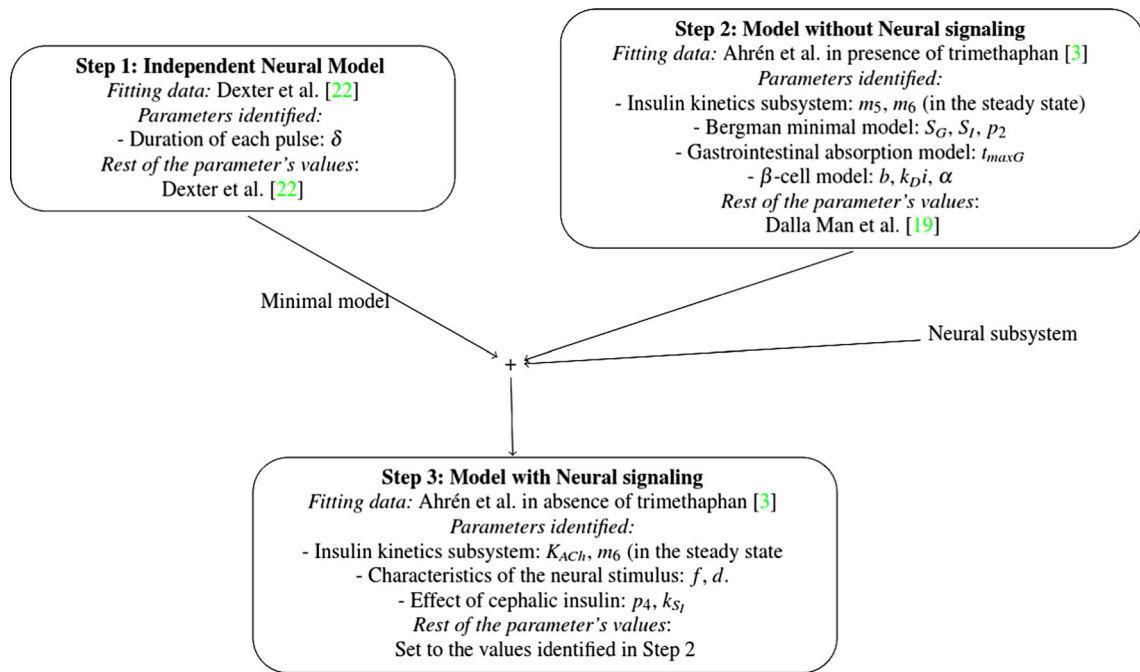
Fig. 5 Summary of the steps carried out for the parameters identification task

Table 1 Constraints used in the parameter identification process and their explanation

Process	Parameter	Constraints	Units	Explanation
Neural model of ACh release	δ	4.2	ms	Absolute refractory period of APs is 1 ms and the maximum duration 5 ms [33]
Bergman minimal model (extended)	p_2	0.01–0.1	min^{-1}	Covers the great variability of values reported in the literature [20, 40, 59]
	S_{Ib}	$(0.66 - 6.79) \cdot 10^{-4}$	min^{-1} per $\mu mol/mL$	Reported by Bergman et al. [11]
	S_G	0.002-0.039	min^{-1}	Covers the range reported by Dalla Man et al. [20] and Steil et al. [44]
Gastrointestinal absorption model	$t_{\max G}$	35–45	min	Cover the value reported by Hovorka et al. [31]
Insulin secretion	k_{Di}	1–3	$pmol/kg$ per mg/dL	Covers the values reported by Dalla Man et al. [19]
	α	0.01–0.5	min^{-1}	Covers the values reported by Dalla Man et al. [19]
	β	0.1–0.2	$pmol/kg$ per mg/dL	Covers the values reported by Dalla Man et al. [19]
Insulin kinetics	m_5	0.015–0.025	$min\,kg/pmol$	Covers the values reported by by Dalla Man et al. [19] and to ensure stability in the steady state
	m_6	0.6–0.7	$min\,kg/pmol$	Covers the values reported by by Dalla Man et al. [19] and to ensure stability in the steady state
Neural stimulus	d	0.5–3	min	No literature found.
	f	0.25–25	Hz	Range reported by Holst et al. [30]
Cephalic insulin release	K_{ACh}	0.1–5	$pmol/kg$ per nM	–
Action of cephalic insulin	p_4	0.005–0.5	min^{-1}	–
	k_{S_I}	$1 \cdot 10^{-5} - 0.1$	$\frac{L\,kg}{pmol^2}$	–

Table 2 Model parameters

Process	Parameter	Value	Units
Neural model of ACh release	K_D	$0.00139^\dagger$	min^{-1}
	K_R	$0.0035^\dagger$	min^{-1}
	ρ	$0.6^\dagger$	$Dimensionless$
	m	$55^\dagger$	nM
	δ	4.2	ms
Bergman minimal model (meal extended)	p_2	0.094	min^{-1}
	S_{Ib}	$6 \cdot 10^{-4}$	min^{-1} per $\mu mol/mL$
	S_G	0.0104	min^{-1}
	V_G	1.88^*	dL/kg
Gastrointestinal absorption model	A_g	$0.85^\star$	Dimensionless
	t_{maxG}	40	min
Insulin secretion	γ	0.5^*	min^{-1}
	k_{Di}	1.54	$pmol/kg$ per mg/dL
	α	0.29	min^{-1}
	β	0.18	$pmol/kg$ per mg/dL
Insulin kinetics	V_I	0.05^*	L/kg
	m_1	0.19^*	min^{-1}
	m_2	0.48^*	min^{-1}
	m_4	0.194^*	min^{-1}
	m_5	0.023	$min\ kg/pmol$
	m_6	0.67	$Dimensionless$
	HE_b	0.6^*	$Dimensionless$
Neural stimulus	d	0.96	min
	f	20	Hz
Cephalic insulin release (cephalic phase)	K_{ACh}	3.17	$pmol/kg$ per nM
Action of cephalic insulin	p_4	0.01	min^{-1}
	k_{S_I}	$9.3 \cdot 10^{-5}$	$\frac{L\ kg}{pmol^2}$

*Values taken from [19], †values taken from [22], *values taken from [31]

10 Hz and a total duration of the train of pulses of 15 s was modeled. It can be clearly seen how the concentration of ACh in the interstitial space increases until reaching a plateau level with some ripple as long as the stimulus was present and decreases exponentially afterwards.

3.2 Complete model identification

All the parameters identified for each biological process can be found in Table 2. Figure 7 shows graphically the fitting of the model in absence (Fig. 7a) and presence (Fig. 7b) of the neural control to the corresponding experimental data. The quality of the fitting regarding the glucose profiles is CV = 10.2% and CV = 5.1% in presence and absence of CPIR, respectively. For the profiles of plasma insulin the obtained fitting errors are CV = 8.4% and CV = 6.5% in presence and absence of CPIR, respectively.

3.3 Impact of the CIPR

A comparison between the postprandial glucose and insulin profiles obtained in presence and absence of the neural contribution is depicted in Fig. 8. The temporal evolution of the insulin sensitivity as a result of the neural control is depicted as well, showing a peak at 17 min after meal intake and progressively decreasing with time afterwards. The amount of plasma insulin secreted during the cephalic phase (incremental area under the curve $iAUC_{CPIR}$) corresponds to a 0.84% of the total plasma insulin secreted in the considered interval (from 0 to 140 min).

Table 3 presents the iAUC of the insulin and glucose profiles obtained in presence and absence of the neural contribution and reports the percentage of reduction of the postprandial plasma levels (19.6% and 24.6% of reduction for postprandial levels of plasma glucose and insulin respectively).
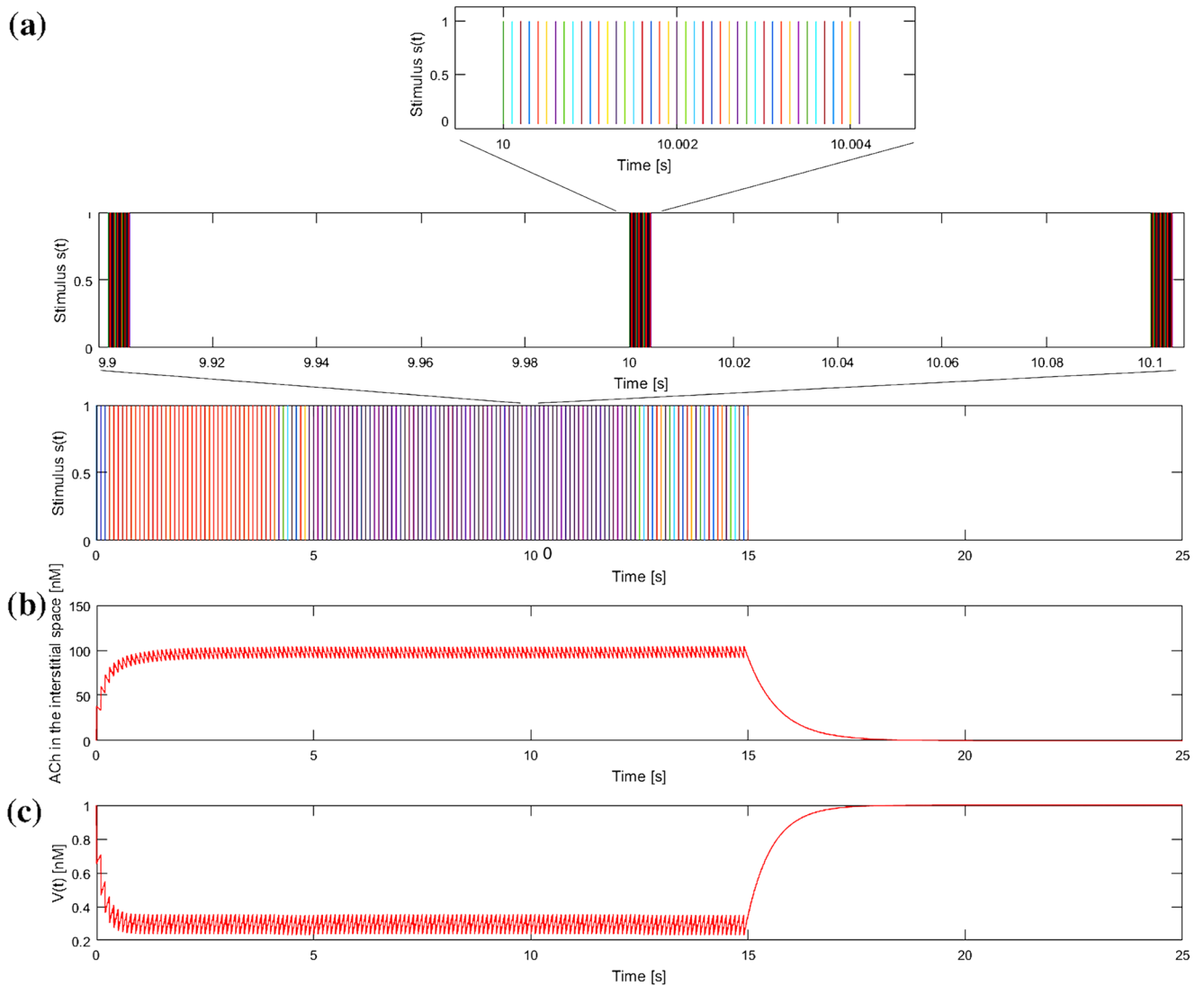
Fig. 6 Neural model of ACh release. **a** Neural stimulus of 10 Hz and 15 s of overall duration and zoom to visualize the train of pulses and its discretization. **b** Profile of ACh concentration in the interstitial space. **c** Profile of vesicles secretion (V(t)) from the nerve terminals

4 Discussion

The proposed model closely replicates the characteristics of the CPIR reported in literature. Firstly, the peak of cephalic insulin release shows a maximum at 5.5 min after meal ingestion, which is within the interval of 3–6 min previously reported in experimental studies [47, 49, 52]. Secondly, it represents approximately 0.84% of the total insulin secreted, which is slightly lower than the previously reported range of 1 ± 3 % [47]. However, it is in agreement with the values reported by Ahrén et al. (0.80 ± 0.22%) [3], whose experimental results were used for the model's identification. In addition, the insulin sensitivity shows a maximum at 17 min after meal intake due to the enhanced action of insulin on hepatic glucose uptake, being also consistent

with previous research [3, 37]. From Fig. 8 and Table 3, it can be seen that inclusion of the small amount of neurally mediated pre-absorptive insulin has a powerful and essential effect in reducing postprandial plasma glucose and insulin levels after the meal intake. This outcome describes the causal inverse relationship between the neurally mediated pre-absorptive insulin and the postprandial hyperglycemia and hyperinsulinemia reported by previous studies [3, 21, 47, 53]. As a result, the proposed neural model of pre-absorptive insulin secretion seems to capture well the physiological effect of the cephalic insulin on hepatic glucose metabolism.

However, the lack of knowledge regarding the neural stimulation of the endocrine pancreas hinders the development of comprehensive mathematical models of its
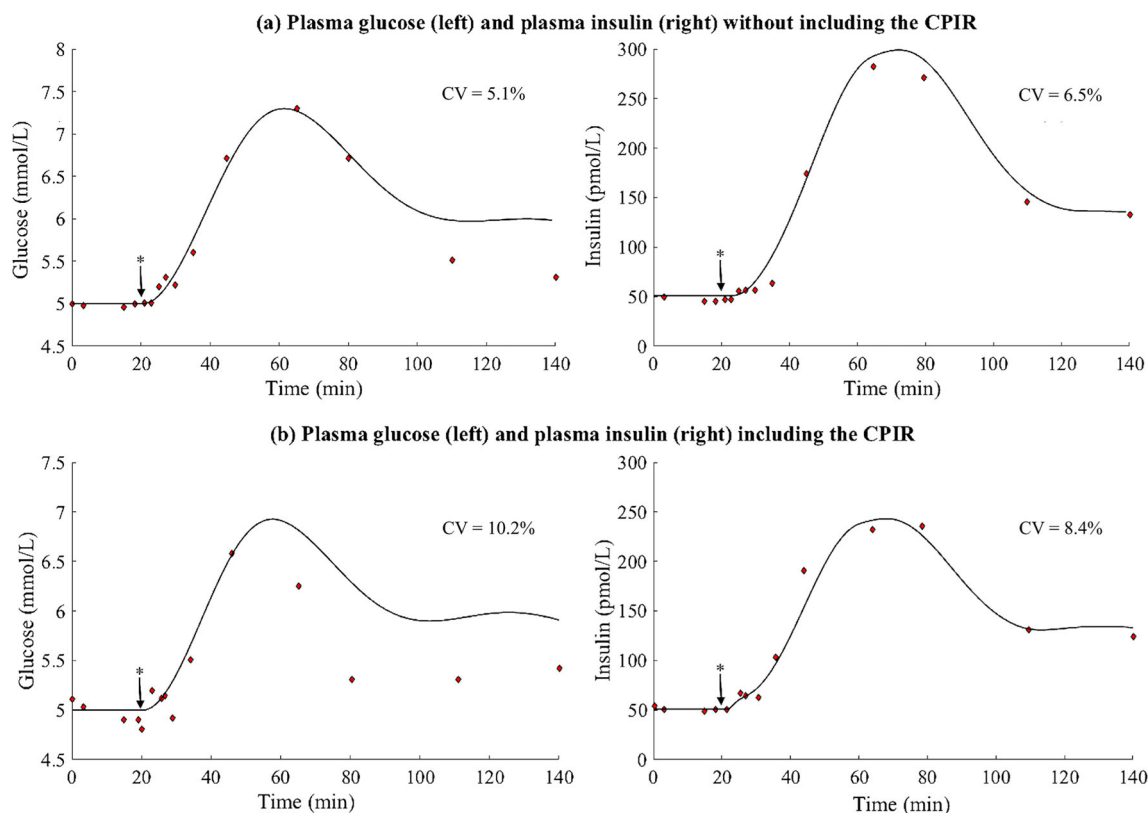
Fig. 7 Comparison of the results of the fitted model with the experimental data. **a** Metabolic model without neural control. **b** Metabolic model including the neural control. Left: Glucose profile. Right: Insulin profile. Model results (continuous line) and fitting data set (red points). The model parameters reported in Table 2 were used. Meal time (*), occurs 20 min after the beginning of the simulation

behavior. In this study, we assumed that the vagus nerve's terminals in different organs have similar kinetics of ACh secretion. Despite appearing to be numerically valid because it allows an accurate representation of the characteristics of the CPIR, it does not represent the real neural-pancreatic interaction. In addition, the CIPR on humans is highly dependent on the type, intensity, and duration of the stimuli [9, 48, 51]. Therefore, further experimental research is needed to identify the characteristics of the nervous signals to the pancreas and their relation with the meal type and size [27].

Moreover, scarcity of large and complete experimental data sets complicates the development of an accurate model in some aspects. Firstly, experimental studies have reported high variability in the pre-absorptive phase of insulin secretion among individuals [10, 47]. Consequently, the mean profile of only six healthy subjects will probably not reflect this intra-subject variability. Secondly, the degrees of freedom of the model was very large to allow an adequate identification of the parameters. Even though the step-wise strategy was implemented to reduce the number of simultaneously estimated

parameters, it is well known that modeling with insufficient data generally leads to over-fitting, and therefore poor generalization. Hence, experimental data describing each subsystem in the presence and absence of neural regulation is needed to accurately identify and validate this model.

Finally, the neural control of the pancreatic secretion was modeled by considering the cholinergic signaling mechanisms. Disregarding the non-cholinergic pathways might also account for some uncertainties in the results. However, the degree of uncertainty is unclear because of the discrepancies found in the literature regarding the impact of atropine on the inhibition of the CPIR. In fact, some studies report an effective action [15, 50]; whereas in others, its effect is lower [3]. These variations have been explained by the use of different experimental conditions, types of food stimuli and gender of subjects (men have been shown to have a higher sensitivity to atropine [3, 50]).

All these limitations might explain the deviations of the model from the experimental data during the postprandial phase, especially regarding the plasma glucose profiles

Fig. 8 Postprandial glucose, insulin, and insulin sensitivity profiles along time in presence and absence of the cephalic phase. **a** Glucose profile. **b** Insulin profile. The small insert depicts the insulin levels corresponding to the cephalic phase (from the ingestion of the meal to 15 min after it). **c** Insulin sensitivity profile. The meal (*) was given 20 min after the beginning of the simulations
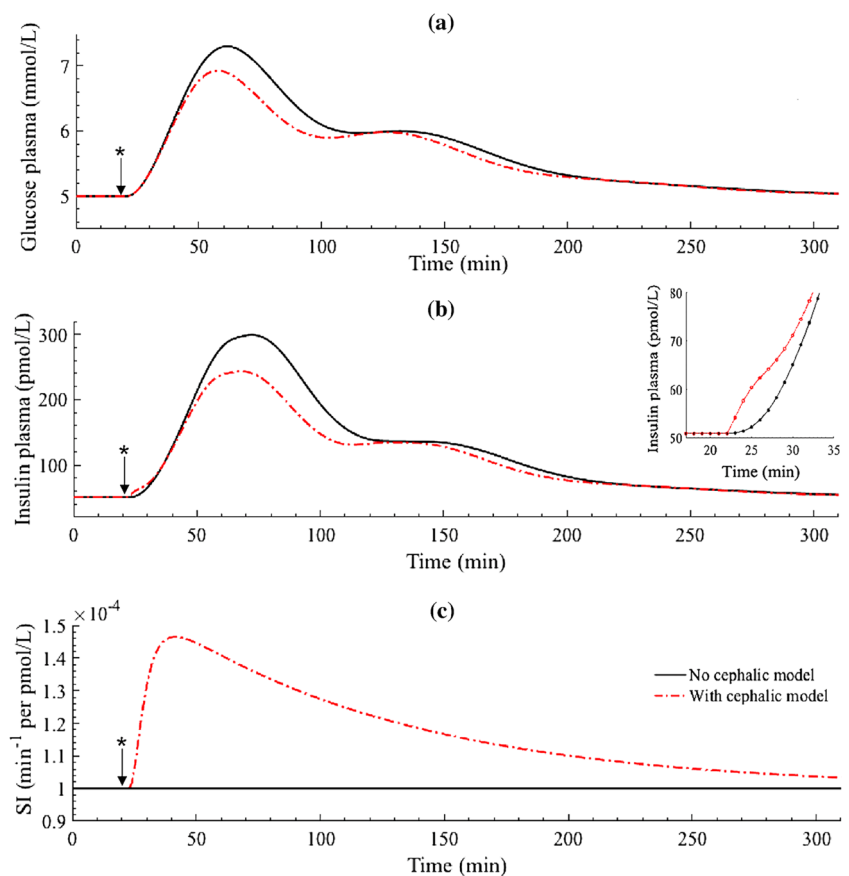
(see left panels in Fig. 7a–b). Despite them, the unified neural-metabolic successfully reproduce the characteristics of the CPIR and gives insight into the dynamics of its postprandial effects. This finding, while preliminary, suggests that existing models of glucose homeostasis, which currently neglect the neural contribution, would benefit from acquiring a better understanding of the physiological basis of the interaction between the brain and the pancreas.

Table 3 Relative decrease in postprandial glucose and insulin plasma levels for each cephalic model with respect to the absence of neural control

	Without neural control	With neural control	% of reduction
iAUC postprandial plasma insulin	15.4 nmol/L	11.6 nmol/L	24.6%
iAUC postprandial plasma glucose	174.8 mmol/L	140.1 mmol/L	19.6%

5 Conclusion

To the best of our knowledge, this work is the first attempt at defining a physiological neurally mediated metabolic model in healthy subjects. In it, the pancreas secretion is no longer controlled solely by hormones and metabolites, as current models do, but also includes the essential effect of the neural control in achieving an optimal glucose control.

Notwithstanding the limitations of the proposed model, the results closely represents the physiological effect of the cephalic insulin, as well as the glucose and insulin profiles in the presence of the neural innervation observed in healthy people. Hence, it presents a more detailed physiological model of the complex regulation of the healthy endocrine pancreas. This is important as *in silico* models provide a good platform to optimize systems and provide insight without the need for initial clinical validation on animals [23, 38].

In addition, it lays the foundation for the development of physiological models that reproduce to a great extent the complex regulation of glucose homeostasis in people with diabetes. This will allow existing simulators of diabetes

mellitus to provide improved environments for testing treatments and monitoring interventions [18, 54]. It also opens the door to new approaches for the design of a bio-inspired artificial pancreas for type 1 diabetes treatment [29, 39], by completely closing the controlling loop using the neural signals to inform the controller about meal ingestion information.

In conclusion, the proposed work gives insight into the physiological basis of the nervous control of the pancreatic secretion and suggests the potential benefit of considering the neural information for restoring glucose control in people with diabetes.

Compliance with Ethical Standards

Publisher's note Springer Nature remains neutral with regard to jurisdictional claims in published maps and institutional affiliations.

References

1. Ahrén BO, Taborsky GJ Jr (1986) The mechanism of vagal nerve stimulation of glucagon and insulin secretion in the dog. Endocrinology 118:1551–1557. https://doi.org/10.1210/endo-118-4-1551

2. Ahrén B (2000) Autonomic regulation of islet hormone secretion - Implications for health and disease. Diabetologia 43:393–410. https://doi.org/10.1007/s001250051322

3. Ahrén B, Holst JJ (2001) The cephalic insulin response to meal ingestion in humans is dependent on both cholinergic and noncholinergic mechanisms and is important for postprandial glycemia. Diabetes 50:1030–1038

4. Ahrén B, Veith RC, Taborsky GJ (1987) Sympathetic nerve stimulation versus pancreatic norepinephrine infusion in the dog: 1) effects on basal release of insulin and glucagon. Endocrinology 121:323–331. https://doi.org/10.1210/endo-121-1-323

5. AmsterCHEM (2017) ScanIt. https://www.amsterchem.com/scanit.html. Accessed 20 Aug 2017

6. Andersson P, Holst J, JÄrhult J (1982) Effects of adrenergic blockade on the release of insulin, glucagon and somatostatin from the pancreas in response to splanchnic nerve stimulation in cats. Acta Physiol 116:403–409

7. Auger A, Hansen N (2005) A restart CMA evolution strategy with increasing population size. In: 2005 IEEE congress on evolutionary computation. IEEE, pp 1769–1776

8. Babic T, Travagli RA (2016) Neural control of the pancreas. Pancreapedia Exocrine Pancreas Knowl Base. https://doi.org/10.3998/panc.2016.27

9. Bellisle F, Louis-Sylvestre J, Demozay F, Blazy D, Le Magnen J (1983) Reflex insulin response associated to food intake in human subjects. Physiol Behav 31:515–521

10. Bellisle F, Louis-Sylvestre J, Demozay F, Blazy D, Le Magnen J (1985) Cephalic phase of insulin secretion and food stimulation in humans: a new perspective. Am J Physiol 249:E639–45. https://doi.org/10.1152/ajpendo.1985.249.6.E639

11. Bergman RN, Ider YZ, Bowden CR, Cobelli C (1979) Quantitative estimation of insulin sensitivity. Am J Physiol 236:E667–77. https://doi.org/10.1152/ajpendo.1979.236.6.E667

12. Bergman RRN, Miller RER (1973) Direct enhancement of insulin secretion by vagal stimulation of the isolated pancreas. Am J Physiol Content 225:481–486. https://doi.org/10.1152/ajplegacy.1973.225.2.481

13. Bernard C (1865) Leçons de physiologie expérimentale appliquée à la médecine: Cours de semestre d'hiver 1854–1855. Bailliere

14. Berthoud HR, Powley TL (1990) Identification of vagal preganglionics that mediate cephalic phase insulin response. Am J Physiol 258:R523–30. https://doi.org/10.1152/ajpregu.1990.258.2.R523

15. Berthoud HR, Bereiter DA, Trimble ER, Siegel EG, Jeanrenaud B (1981) Cephalic phase, reflex insulin secretion neuroanatomical and physiological characterization. Diabetologia 20:393–401. https://doi.org/10.1007/BF00254508

16. Breda E, Cavaghan MK, Toffolo G, Polonsky KS, Cobelli C (2001) Oral glucose tolerance test minimal model indexes of β-cell function and insulin sensitivity. Diabetes 50:150–158

17. Chandra R, Liddle RA (2014) Recent advances in the regulation of pancreatic secretion. Curr Opin Gastroenterol 30:490

18. Dalla Man C, Micheletto F, Lv D, Breton M, Kovatchev B, Cobelli C (2014) The UVA/PADOVA type 1 diabetes simulator: new features. J Diabetes Sci Technol 8:26–34. https://doi.org/10.1177/1932296813514502

19. Dalla Man C, Rizza RA, Cobelli C (2007) Meal simulation model of the glucose-insulin system. IEEE Trans Biomed Eng 54:1740–1749

20. Dalla Man C, Yarasheski KE, Caumo A, Robertson H, Toffolo G, Polonsky KS, Cobelli C (2005) Insulin sensitivity by oral glucose minimal models: validation against clamp. Am J Physiol Metab 289:E954–E959. https://doi.org/10.1152/ajpendo.00076.2005

21. Del Prato S, Tiengo A (2001) The importance of first-phase insulin secretion: implications for the therapy of type 2 diabetes mellitus. Diabetes Metab Res Rev 17:164–174

22. Dexter F, Levy MN, Rudy Y (1989) Mathematical model of the changes in heart rate elicited by vagal stimulation. Circ Res 65:1330–1339

23. Doke SK, Dhawale SC (2015) Alternatives to animal testing: a review. Saudi Pharm J SPJ Off Publ Saudi Pharm Soc 23:223–9. https://doi.org/10.1016/j.jsps.2013.11.002

24. Ewing G (2010) Mathematical modeling the neuroregulation of blood pressure using a cognitive top-down approach. N Am J Med Sci 2:341–352. https://doi.org/10.4297/najms.2010.2341

25. Frohman LA, Ezdinli EZ, Javid R (1967) Effect of vagotomy and vagal stimulation on insulin secretion. Diabetes 16:443–448. https://doi.org/10.2337/DIAB.16.7.443

26. Gilon P, Henquin J-C (2001) Mechanisms and physiological significance of the cholinergic control of pancreatic β-cell function. Endocr Rev 22:565–604

27. Güemes A, Georgiou P (2018) Review of the role of the nervous system in glucose homoeostasis and future perspectives towards the management of diabetes. Bioelectron Med 4(1):9

28. Hansen N (2006) The CMA evolution strategy: a comparing Review. In: Lozano JA, Larrañaga P, Inza I, Bengoetxea E (eds) Towards a new evolutionary computation. Studies in Fuzziness and Soft Computing, vol 192. Springer, Berlin, Heidelberg

29. Herrero P, Georgiou P, Oliver N, Reddy M, Johnston D, Toumazou C (2013) A composite model of glucagon-glucose dynamics for in silico testing of bihormonal glucose controllers. J Diabetes Sci Technol 7:941–951. https://doi.org/10.1177/1932296813007000416

30. Holst JJ, Gronholt R, Schaffalitzky de Muchadell OB, Fahrenkrug J (1981) Nervous control of pancreatic endocrine secretion in pigs (I). Acta Physiol Scand 111:1–7

31. Hovorka R, Canonico V, Chassin LJ, Haueter U, Massi-Benedetti M, Federici MO, Pieber TR, Schaller HC, Schaupp L, Vering T, Others (2004) Nonlinear model predictive control of glucose concentration in subjects with type 1 diabetes. Physiol Meas 25:905

32. Ionescu E, Rohner-Jeanrenaud F, Berthoud H-R, Jeanrenaud B (1983) Increases in plasma insulin levels in response to electrical stimulation of the dorsal motor nucleus of the vagus nerve. Endocrinology 112:904–910

33. Kandel ER, Schwartz JH, Jessell TM, Siegelbaum SA, Hudspeth AJ (2000) Principles of neural science, 5th edn. McGraw-hill

34. Luzi L, DeFronzo RA (1989) Effect of loss of first-phase insulin secretion on hepatic glucose production and tissue glucose disposal in humans. Am J Physiol 257:E241–6. https://doi.org/10.1152/ajpendo.1989.257.2.E241

35. Meyers EE (2016) Afferent vs efferent cervical vagal nerve stimulation: effects on blood glucose, insulin, and glucagon concentrations in rats

36. Osundiji MA, Evans ML (2013) Brain control of insulin and glucagon secretion. Endocrinol Metab Clin North Am 42:1–14. https://doi.org/10.1016/j.ecl.2012.11.006

37. Pagliassotti MJ, Holste LC, Moore MC, Neal DW, Cherrington AD (1996) Comparison of the time courses of insulin and the portal signal on hepatic glucose and glycogen metabolism in the conscious dog. J Clin Invest 97:81–91. https://doi.org/10.1172/JCI118410

38. Radenković M, Stojanović M, Prostran M (2016) Experimental diabetes induced by alloxan and streptozotocin: the current state of the art. J Pharmacol Toxicol Methods 78:13–31. https://doi.org/10.1016/J.VASCN.2015.11.004

39. Reddy M, Herrero P, El Sharkawy M, Pesl P, Jugnee N, Thomson H, Pavitt D, Toumazou C, Johnston D, Georgiou P, Oliver N, Others (2014) Feasibility study of a bio-inspired artificial pancreas in adults with type 1 diabetes. Diabetes Technol Ther 16:550–557. https://doi.org/10.1089/dia.2014.0009

40. van Riel N (2004) Minimal models for glucose and insulin kinetics; a Matlab implementation. Eindhoven Univ Technol: 1–12. https://doi.org/10.13140/2.1.1766.7361

41. Rodriguez-Diaz R, Caicedo A (2014) Neural control of the endocrine pancreas. Best Pract Res Clin Endocrinol Metab 28:745–756. https://doi.org/10.1016/J.BEEM.2014.05.002

42. Rosario W, Singh I, Wautlet A, Patterson C, Flak J, Becker TC, Ali A, Tamarina N, Philipson LH, Enquist LW, Others (2016) The brain–to–pancreatic islet neuronal map reveals differential glucose regulation from distinct hypothalamic regions. Diabetes 65:2711–2723

43. Rybak IA, Molkov YI, Paton JFR, Abdala APL, Zoccal DB (2011) Modeling respiratory-sympathetic interactions and baroreceptor reflex control. Semant Sch 1–12

44. Steil GM, Volund A, Kahn SE, Bergman RN (1993) Reduced sample number for calculation of insulin sensitivity and glucose effectiveness from the minimal model. Suitability for use in population studies. Diabetes 42:250–6. https://doi.org/10.2337/DIAB.42.2.250

45. Taborsky GJ (2011) Insulin and glucagon secretion in vivo and its neural control. Compr Physiol. Supplement 21: handbook of physiology, the endocrine system, the endocrine pancreas and regulation of metabolism, pp 153–176. https://doi.org/10.1002/cphy.cp070206

46. Teff K (2000) Nutritional implications of the cephalic-phase reflexes: endocrine responses. Appetite 34:206–213

47. Teff KL (2011) How neural mediation of anticipatory and compensatory insulin release helps us tolerate food. Physiol Behav 103:44–50

48. Teff KL (2010) Cephalic phase pancreatic polypeptide responses to liquid and solid stimuli in humans. Physiol Behav 99:317–323. https://doi.org/10.1016/J.PHYSBEH.2009.1009

49. Teff KL, Mattes RD, Engelman K, Mattern J (1993) Cephalic-phase insulin in obese and normal-weight men: relation to postprandial insulin. Metabolism 42:1600–1608. https://doi.org/10.1016/0026-0495(93)90157-J

50. Teff KL, Townsend RR (1999) Early phase insulin infusion and muscarinic blockade in obese and lean subjects. Am J Physiol Integr Comp Physiol 277:R198–R208. https://doi.org/10.1152/ajpregu.1999.277.1.R198

51. Teff KL, Devine J, Engelman K (1995) Sweet taste: effect on cephalic phase insulin release in men. Physiol Behav 57:1089–1095

52. Teff KL, Engelman K (1996) Oral sensory stimulation improves glucose tolerance in humans: effects on insulin, C-peptide, and glucagon. Am J Physiol Integr Comp Physiol 270:R1371–R1379

53. Teff KL, Petrova M, Havel PJ, Townsend RR (2007) 48-h glucose infusion in humans: effect on hormonal responses, hunger and food intake. Physiol Behav 90:733–743. https://doi.org/10.1016/j.physbeh.2006.12.013

54. The Epsilon Group (TEG) (2017) DMMS for Research. https://tegvirginia.com/software/dmms-r/. Accessed 29 Nov 2017

55. Thorens B (2011) Brain glucose sensing and neural regulation of insulin and glucagon secretion. Diabetes, Obes Metab 13:82–88. https://doi.org/10.1111/j.1463-1326.2011.01453.x

56. Thorens B (2014) Neural regulation of pancreatic islet cell mass and function. Diabetes, Obes Metab 16:87–95. https://doi.org/10.1111/dom.12346

57. Toffolo G, Breda E, Cavaghan MK, Ehrmann DA, Polonsky KS, Cobelli C (2001) Quantitative indexes of β-cell function during graded up& amp;down glucose infusion from C-peptide minimal models. Am J Physiol Metab 280:E2–E10. https://doi.org/10.1152/ajpendo.2001.280.1.E2

58. Veedfald S, Plamboeck A, Deacon CF, Hartmann B, Knop FK, Vilsbøll T, Holst JJ (2016) Cephalic phase secretion of insulin and other enteropancreatic hormones in humans. Am J Physiol Liver Physiol 310:G43–G51. https://doi.org/10.1152/ajpgi.00222.2015

59. Vilhjalmsdottir EO (2013) Deterministic and Stochastic Modeling of Insulin Sensitivity. Master's Thesis

60. Warner HR, Others (1969) Effect of combined sympathetic and vagal stimulation on heart rate in the dog. Circ Res 24:567–573

Amparo Güemes received the B.S. degree in Biomedical Engineering from the Universidad Politécnica de Madrid (UPM), Madrid, Spain, in 2016, and the M.S. degree Biomedical Engineering from Imperial College London (ICL), London, UK, in 2017. She is currently a Ph.D. candidate in the Centre for Bio-Inspired Technology at Imperial College London. Her research interests lie in the fields of neurotechnology and diabetes treatment. In particular, she has worked in the design of physiological models of the pancreas secretion and her PhD is focused on applying bioelectronics medicine as a new therapy to improve diabetes management.

Pau Herrero received the MSc degree in Information Technologies from University of Girona (Spain) in 2002 and the Ph.D. degree in Automation from University of Angers (France) in 2006. He is currently a Research Fellow within the Department of Electrical & Electronic Engineering at Imperial College London. He holds two patents. His main research interest lies in the field of diabetes technology and antimicrobial resistance. In particular, he is involved in the development of an artificial pancreas system and an intelligent decision support system for diabetes management.

Jorge Bondia received an M.Sc. degree in Computer Science in 1994, and the Ph.D. degree in Control Engineering in 2002 both from the Universitat Politècncia de València, Spain. He is a Full Professor since 2017. He has been teaching since 1995 at the Systems Engineering and Control Department, Universitat Politècncia de València on subjects in the fields of automation, control engineering, and biomedical engineering. He develops his research activity as a member of the University Institute of Control Systems and Industrial Computing (Institute ai2), where he started a research line on diabetes technology and the artificial pancreas in 2004. His main research lines are modeling of type 1 diabetes pathophysiology, intra-patient variability and glucose prediction under uncertainty, tools for insulin therapy optimization, and new calibration algorithms for accuracy improvement of continuous glucose monitoring and control algorithms for an efficient and safe artificial pancreas. He has published more than 40 articles on the artificial pancreas and contributed to more than 100 conferences. He is currently the Head of the MEDERI Living Lab at Institute ai2, dedicated to new technologies for chronic diseases, rehabilitation and health education.

Pantelis Georgiou received the M.Eng. degree in electrical and electronic engineering and the Ph.D. degree from Imperial College London (ICL), London, U.K., in 2004 and 2008, respectively. He is currently a Reader with the Department of Electrical and Electronic Engineering, ICL, where he is also the Head of the Bio-Inspired Metabolic Technology Laboratory, Centre for Bio-Inspired Technology. His research includes bio-inspired circuits and systems, CMOS based Lab-on-Chip technologies, and application of microelectronic technology to create novel medical devices. He has made significant contributions to integrated chemical-sensing systems in CMOS, conducting pioneering work on the development of ISFET sensors, which has enabled applications, such as point-of-care diagnostics and semiconductor genetic sequencing and has also developed the first bio-inspired artificial pancreas for treatment of type I diabetes using the silicon-beta cell. He received the IET Mike Sergeant Medal of Outstanding Contribution to Engineering in 2013. He is a member of the IET and serves on the BioCAS and Sensory Systems technical committees of the IEEE CAS Society. He is also the CAS representative on the IEEE Sensors council and the IEEE Distinguished Lecturer in Circuits and Systems.